

NUMERICAL SIMULATION OF TURBULENT FORCED CONVECTION COUPLED TO HEAT CONDUCTION IN SQUARE DUCTS

Gustavo Adolfo Ronceros Rivas

Universidade Federal da Integração Latino-Americana (UNILA)
Engenharia de Energias Renováveis.
Avenida Tancredo Neves, 6731 - Bloco 4, CEP: 85867-970, Foz do Iguaçu - Paraná - Brasil.
gustavo.rivas@unila.edu.br

Ézio Castejon Garcia

Instituto Tecnológico de Aeronáutica (ITA)
Divisão de Engenharia Mecânica e Aeronáutica, Departamento de Energia.
Praça Marechal do Ar Eduardo Gomes, 50 - Vila das acácias, CEP: 12.228-900, SJC - SP - Brasil.
ezio@ita.br

Marcelo Assato

Universidade Federal de Juiz de Fora (UFJF)
Departamento de Engenharia Mecânica.
Rua José Lourenço Kelmer, s/n - Campus Universitário, Bairro São Pedro - CEP: 36036-900, Juiz de fora, MG - Brasil.
marcelo.assato@ufff.edu.br

Abstract. *In the present work, the numerical simulation was adopted to resolve the problem of the turbulent forced convection coupled to heat conduction in a duct of the square cross-section. The governing equations for turbulent convection are the continuity, momentum, and energy equations (Reynolds Averaged Navier Stokes, RANS). These equations are coupled to heat conduction coming through of four plates situated around of the channel flow, the plates are coupled between itself with thermal resistance of ideal contact. Assumptions main in the flow, such as: condition of fully developed turbulent and incompressible flow had been assumed. The comparison way, had been used two turbulent models to resolve the equations of the momentum and one model to resolve the energy equation. That is, to determine the profiles of velocity, the models of turbulence, $k-\varepsilon$ non linear (NLEVM) and Reynolds Stress Model (RSM), this last model simulated in a commercial code, they had been adopted and studied. The fluid temperature field will be determined from of the model Simple Eddy Diffusivity (SED), based in the hypothesis of the Constant turbulent Prandtl number; for the equation of the energy of the fluid had been dimensionless and developed in a code of programming FORTRAN. The models had been validated in base the experimental and numerical results of literature. Finally the results of this investigation allow evaluating the fluid temperature field for different square cross-sectional sections throughout of the direction of the main flow, which is influenced mainly by the temperature distribution in the wall.*

Keywords: *Numerical simulation, turbulent forced convection, square ducts, coupled solid fluid, thermal systems*

1. INTRODUCTION

Square ducts are widely used in heat transfer devices. For example, in compact heat exchangers, gas turbine cooling systems (secondary flows), cooling channels in combustion chambers, nuclear reactors. The forced turbulent heat convection in a square duct is one of the fundamental problems in the thermal science and fluid mechanics. Recently, Qin and Plethter (2006) showed that the Prandtl's secondary flow of the second kind has a significant effect on the transport of heat and momentum as revealed by the recent large eddy simulation (LES). Several experimental and numerical studies have been conducted on turbulent flow through a non-circular duct, namely, (Nikuradse (1926); Gessner and Emery (1976); Gessner and Po (1976); Melling and Whitelaw (1976); Nakayama et al. (1983); Myon and Kobayashi (1991); Assato (2001) and others). Similarly important works in the turbulent heat convection were developed (Launder and Ying (1973); Emery et al. (1980); Hirota et al. (1997); Rokni (2000); Y. Hongxing (2009)) and others). The experimental work of Melling and Whitelaw (1973) shows detailed characteristics of turbulent flow in a rectangular duct where they used a laser-Doppler anemometer to report the axial development of the mean velocity, secondary mean velocity, etc. Nakayama et al. (1983), it shows the analysis the fully developed flow field in ducts of rectangular and trapezoidal cross-sections using a finite-difference method with the model of Launder and Ying (1973). On the other hand, Hirota *et al.* (1997) present an experimental work on the turbulent heat transfer in a square duct, shows detailed characteristics of turbulent flow and temperature field. Likewise, Rokni (1998), in the doctoral thesis achievement a comparison of four different turbulence models for predicting the turbulent Reynolds Stresses and three turbulent heat fluxes models for ducts square. In the turbulence model it is well known that Linear Eddy Viscosity Models (LEVM) can give rise to inaccurate predictions for the Reynolds normal stresses and so that not have the ability to predict secondary flows of the second kind. In spite of that, they are one of the most popular models in the engineering due to its simplicity, good numerical stability and it can be applied to a wide variety of flows. Thus, NLEVM represents a progress of the classical LEVM which permits inequality of the Reynolds normal stresses, a

necessary condition for calculating turbulence-driven secondary flow in non-circular ducts within the relative cost of a two-equation formulation. The model RSM, also called the second order or second moment closure model is very accurate in the calculation of mean flow properties and all Reynolds stresses for many simple and more complex flows including wall jets, asymmetric channel and non-circular duct flows and curved flows, also present, disadvantages, just as, very large computing costs. The SED models for calculated turbulent heat flux have been adopted and studied. The bibliographical revision shows that the majority of the cited works had been previously developed for constant temperatures in the contour. However, in many applications the heat flux and surface temperature are non-uniform around the duct, becoming important the knowledge of the variation of the conductance around of the duct, Kays and Crawford (1980). According to developments performed by Garcia (1996), it is possible to carry out analysis with non-uniform wall temperature boundary conditions. In this case, it is necessary to define a value that represents the mean wall temperatures in a given cross section, " T_{wm} ", in such way, in the present work intended to give a small contribution with respect to the influence the non-uniform wall temperature on the fluid temperature field considering internal flow with fluids air.

2. NOMENCLATURE

c_p	specific heat at constant pressure
D	duct height
D_h	hydraulic diameter, $D_h = 4.A/P_e = 2.L.D/(L + D)$
dP/dz	pressure gradient at z direction (longitudinal axis)
f, C_f	factor of Moody's friction, and Fanning's friction coefficient, respectively.
k_f	fluid thermal conductivity
L	duct width
Nu	Nusselt number
P_e	perimeter
P_k	turbulence production term
Re	Reynolds number
T	temperature
T_b	internal flow bulk temperature
T_{wm}	wall mean temperature
T_1, T_2, T_3 and T_4	temperature distributions at duct wall (bottom, right side, top and left side)
U_b	internal flow bulk velocity
U, V and W	average velocity in the Cartesian plane in the direction x, y and z ; respectively
y^+	dimensionless wall distance

Greek Symbols

α	thermal diffusivity, $\alpha = k_f / (\rho \cdot c_p)$
η	distance normal to the wall
ϕ	dimensionless temperature distribution
μ	dynamic viscosity
μ_t	turbulent viscosity
ρ	density
σ_t	turbulent Prandtl number

3. Mathematical Formulation

3.1. Governing Equations

The Reynolds Averaged Navier Stokes (RANS) equation system is composed of: continuity equation (1), momentum equation (2), energy equation (3) and (4) heat conduction equation.

$$\frac{\partial}{\partial x_j}(U_j) = 0 \quad (1)$$

$$\frac{\partial}{\partial x_j} (U_i U_j) = -\frac{1}{\rho} \frac{\partial P}{\partial x_i} + \frac{1}{\rho} \frac{\partial}{\partial x_j} \left[\mu \left(\frac{\partial U_i}{\partial x_j} + \frac{\partial U_j}{\partial x_i} \right) \right] + \frac{1}{\rho} \frac{\partial}{\partial x_j} (-\rho \overline{u_i' u_j'}) \quad (2)$$

$$\frac{\partial}{\partial x_j} (U_j T_f) = \frac{1}{\rho} \frac{\partial}{\partial x_j} \left[\frac{\mu}{Pr} \frac{\partial T_f}{\partial x_j} + (-\rho \overline{u_j' t'}) \right] \quad (3)$$

$$\frac{\partial}{\partial x_i} \left(k_s \frac{\partial T_w}{\partial x_i} \right) = 0 \quad (4)$$

For analyses of fully developed turbulent flow and heat transfer, the following hypothesis has been adopted: steady state, condition of non-slip on the wall and fluid with constant properties. The turbulent Reynolds stress $(-\rho \overline{u_i' u_j'})$ and the turbulent heat flux $(-\rho \overline{u_j' t'})$ were modeled and solved by algebraic and/or differential expressions.

3.2. Turbulence Models for Reynolds Stresses

3.2.1. Nonlinear Eddy Viscosity Model (NLEVM)

The NLEVM Model to reproduce the tensions of Reynolds, it is necessary to include non-linear terms in the basic constitutive equations. This is done by attempting to capture the sensitivity of the curvatures of the stream lines. This model is based on the initial proposal of Speziale (1987). The Reynolds average equations, Equations (1) to (3), are applied for the device presents in the Figure 1(a) and (b).

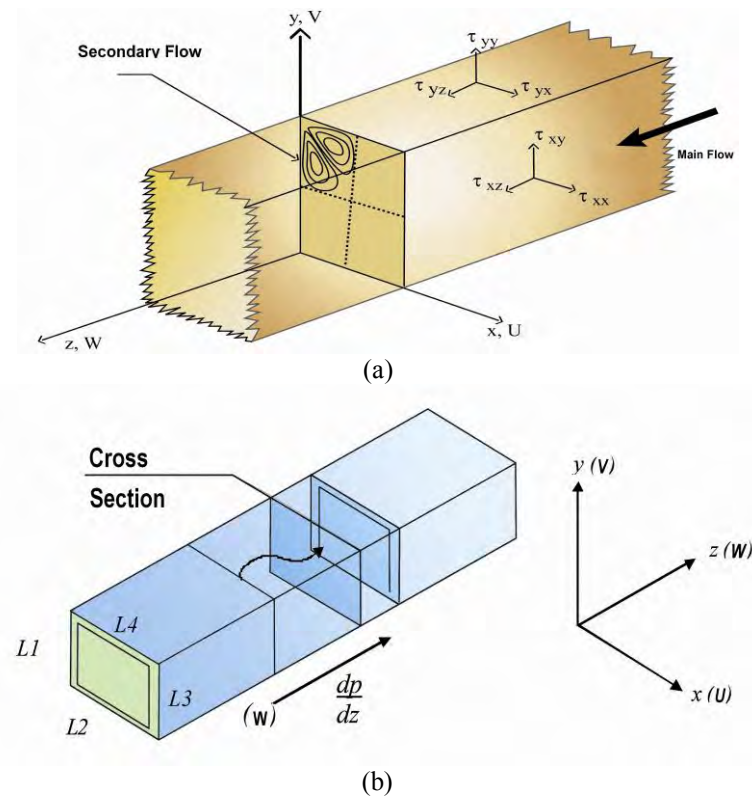


Figure 1: (a) Fully developed turbulent flows in rectangular ducts, (b) Rectangular duct: reference system and transversal section.

The velocity components U and V represent the secondary flow, and the axial velocity component W , the velocity of the main flow. The transport equations in tensorial form for the turbulent kinetic energy, κ , and the rate of dissipation, ε ,

respectively, they are given by:

$$U_i \frac{\partial k}{\partial x_i} = \frac{\partial}{\partial x_i} \left(\frac{\mu_t}{\rho \sigma_k} \frac{\partial k}{\partial x_i} \right) + P_k - \varepsilon \quad (5)$$

$$U_i \frac{\partial \varepsilon}{\partial x_i} = \frac{\partial}{\partial x_i} \left(\frac{\mu_t}{\rho \sigma_\varepsilon} \frac{\partial \varepsilon}{\partial x_i} \right) + c_1 \frac{\varepsilon}{k} P_k - c_2 f_2 \frac{\varepsilon^2}{k} \quad (6)$$

The symbols P_k and μ_t , represent the rate of the turbulent kinetic energy production and the turbulent viscosity, respectively, and thus, we have:

$$P_k = \tau_{ij} \frac{\partial U_i}{\partial x_j}, \mu_t = c_\mu f_\mu \rho \frac{k^2}{\varepsilon} \quad (7)$$

In the present work for NLEVM, the formulations of Low Reynolds Number will be assumed for wall treatment. The damping functions f_2 and f_μ is observed in the Equations (6) and (7) and shown in the Table 1. These functions and the constant C_1 and C_2 have been used together with the equations κ - ε , the subscribed letter P refers to the nodal point near to the wall. Thus U_P and k_P are the values of the velocity and kinetic energy in this point, respectively. The constant c_μ , c_1 , c_2 , σ_k and σ_ε they adopt the values of 0.09; 1.5; 1.9; 1.4 e 1.3; respectively. The new constitutive relation for the tensions of Reynolds in the model NLEVM, assumed in the thesis of Assato, 2001, is given by:

$$\tau_{ij} = (\mu_t S_{ij})^L + \left(c_{1NL} \mu_t \frac{k}{\varepsilon} [S_{ik} S_{kj} - \frac{1}{3} S_{kl} S_{kl} \delta_{ij}] \right)^{NL} \quad (8)$$

This expression shows that the second term of the right side of the Equation (8), represents the nonlinear term added the original constitutive relation. This quadratic term represents the degree of anisotropy between the normal tensions of Reynolds, which makes it possible to predict the presence of the secondary flow in non circular ducts. The values of c_{1NL} proposed by Speziale (1987) are equal to 1.68. Here, c_{1NL} will be analyzed and will adopt values for the formulation of Low Reynolds Numbers. The tensions of Reynolds, normal and shear, are presented in the Equations (9), (10) and (10), are expressed as:

$$\tau_{xx} = c_{1NL} \mu_t \frac{k}{\varepsilon} \left[\frac{1}{3} \left(\frac{\partial W}{\partial x} \right)^2 - \frac{2}{3} \left(\frac{\partial W}{\partial y} \right)^2 \right]; \tau_{yy} = c_{1NL} \mu_t \frac{k}{\varepsilon} \left[\frac{1}{3} \left(\frac{\partial W}{\partial y} \right)^2 - \frac{2}{3} \left(\frac{\partial W}{\partial x} \right)^2 \right] \quad (9)$$

$$\tau_{xy} = c_{1NL} \mu_t \frac{k}{\varepsilon} \left[\frac{\partial W}{\partial x} \frac{\partial W}{\partial y} \right]; \tau_{xz} = \mu_t \frac{\partial W}{\partial x}; \tau_{yz} = \mu_t \frac{\partial W}{\partial y} \quad (10)$$

The following differences for the normal tensions of Reynolds are presented and have been observed for this type of flow.

$$(\tau_{yy} - \tau_{xx}) = c_{1NL} \mu_t \frac{k}{\varepsilon} \left[\left(\frac{\partial W}{\partial y} \right)^2 - \left(\frac{\partial W}{\partial x} \right)^2 \right] \quad (11)$$

In such a way in Equation (7), including the derivatives above the tensions of Reynolds, the turbulence production term, is expressed as:

$$P_k = \tau_{xz} \frac{\partial W}{\partial x} + \tau_{yz} \frac{\partial W}{\partial y} \quad (12)$$

3.2.2. Reynolds Stress Model (RSM)

The most complex turbulence is the Reynolds Stress Model (RSM), also called of second order, it involves calculations of the tensions of Reynolds in an individual form, $\overline{\rho u'_i u'_j}$, used for this differential equations of transport. The individual Reynolds tensions are utilized to close the average Reynolds equations of the momentum. This model has shown superiority regarding the models of two equations in complex flows that involve swirl, rotation, etc. The exact equations of transport for the Reynolds tensions, $\overline{\rho u'_i u'_j}$, can be written as follows:

$$\begin{aligned} \frac{\partial}{\partial t}(\overline{\rho u'_i u'_j})(a) + \frac{\partial}{\partial x_k}(\overline{\rho u'_k u'_i u'_j})(b) = & -\frac{\partial}{\partial x_k} \left[\overline{\rho u'_i u'_j u'_k} + \overline{p(\delta_{kj} u'_i + \delta_{ik} u'_j)} \right](c) + \\ \frac{\partial}{\partial x_k} \left[\mu \frac{\partial}{\partial x_k} (\overline{u'_i u'_j}) \right](d) - \rho \left(\overline{u'_i u'_k} \frac{\partial u'_j}{\partial x_k} + \overline{u'_j u'_k} \frac{\partial u'_i}{\partial x_k} \right)(e) - \rho \beta (g_i \overline{u'_j \theta} + g_j \overline{u'_i \theta})(f) & (13) \\ p \left(\frac{\partial u'_i}{\partial x_j} + \frac{\partial u'_j}{\partial x_i} \right)(g) - 2\mu \frac{\partial u'_i}{\partial x_k} \frac{\partial u'_j}{\partial x_k}(h) - 2\rho \Omega_k (u'_j u'_m \varepsilon_{ikm} + u'_i u'_m \varepsilon_{jkm})(i) + S(j) & \end{aligned}$$

Where the respective letters represent: (a) local derivative of the time; (b) C_{ij} convection; (c) $D_{T,ij}$ Turbulent diffusion; (d) $D_{L,ij}$ molecular diffusion; (e) P_{ij} production Term of tensions; (f) G_{ij} buoyancy production Term; (g) ϕ_{ij} Term of pressure-tension (redistribution); (h) ε_{ij} Term of dissipation; (i) F_{ij} Term production for the rotation system; (j) S_j Source term; The terms of the exact equations, presented previously, C_{ij} , $D_{L,ij}$, P_{ij} and F_{ij} do not require modeling. However, the terms $D_{T,ij}$, G_{ij} , ϕ_{ij} and ε_{ij} need to be modeled to close the equations. For the present analysis, the model LRR (Launder, Reece e Rodi, 1975) is chosen, which assumes that the correlation velocity pressure is a linear function of the anisotropy tensor LRR in the phenomenology of the redistribution, ϕ_{ij} . For the treatment of the wall, it is also assumed the Low Reynolds numbers and the periodic conditions, Rokni (1996). This model had been simulated in the commercial code Fluent 6.3.

3.3 Turbulence Models for Turbulent Heat Flux

3.3.1. Simple Eddy Diffusivity (SED)

This method is based on the Boussinesq viscosity model. The turbulent diffusivity for the energy equation can be expressed as: $\alpha_t = \frac{\mu_t}{\rho \sigma_t}$, where the turbulent Prandtl number σ_t needs to be given. The SED Model assumes that the turbulent Prandtl number is constant in the entire region, for the air σ_t it assumes values of 0.89, independent on the wall proximity effect.

$$\overline{\rho u'_j t} = -\frac{\mu_t}{\sigma_T} \frac{\partial T_f}{\partial x_j} \quad (14)$$

3.3.2. Generalized Gradient Diffusion Hypothesis (GGDH)

Daly and Harlow (1970) present the following formulation to the turbulent heat flux:

$$\overline{\rho u'_j t} = -\rho C_t \frac{k}{\varepsilon} \left(\overline{u'_j u'_k} \frac{\partial T_f}{\partial x_k} \right) \quad (15)$$

G. Rivas, E. Garcia and M. Assato
 Numerical Simulation of Turbulent Forced Convection Coupled to Heat Conduction in Square Ducts

The constant C_t , assuming the value of 0.3, is adopted. The main advantage of this model is that it considers the anisotropic behavior of the fluid heat transport in ducts.

3.3.3. Dimensionless Energy Equation for SED and GGDH Models

For a given cross section of area “ A ”, it is possible to define a mean velocity “ U_b ” and a bulk temperature “ T_b ”, express as:

$$U_b = \frac{1}{A} \iint W \cdot dx \cdot dy \quad \text{and} \quad T_b = \frac{\int W \cdot T_f \cdot dA}{U_b \cdot A} = \frac{1}{AU_b} \iint W \cdot T_f \cdot dx \cdot dy \quad (16) \text{ and } (17)$$

Kays and Crawford (1980) developed an applicable formulation to rectangular cross section ducts. They considered the boundary conditions with prescribed uniform wall temperatures at the cross section, and along the duct length. According to developments performed by Garcia (1996), it is possible to carry out analysis with non-uniform wall temperature boundary conditions. In this case, it is necessary to define a value that represents the mean wall temperatures in a given cross section, “ T_{wm} ”, given as:

$$T_{wm} = \frac{\left[\frac{1}{L} \cdot \int_0^L T_1(0, y) \cdot dy + \frac{1}{D} \cdot \int_0^D T_2(x, 0) \cdot dx + \frac{1}{L} \cdot \int_0^L T_3(D, y) \cdot dy + \frac{1}{D} \cdot \int_0^D T_4(x, L) \cdot dx \right]}{2(L + D)} \quad (18)$$

It is possible to develop a formula similar to Kays and Crawford (1980), the new expression for the turbulent energy equation, is presented as:

$$U \frac{\partial T_f}{\partial x} + V \frac{\partial T_f}{\partial y} + W \frac{\partial T_f}{\partial z} - \left[\frac{\partial}{\partial x} \left(\alpha \frac{\partial T_f}{\partial x} - \overline{ut} \right) + \frac{\partial}{\partial y} \left(\alpha \frac{\partial T_f}{\partial y} - \overline{vt} \right) + \frac{\partial}{\partial z} \left(\alpha \frac{\partial T_f}{\partial z} - \overline{wt} \right) \right] = 0 \quad (19)$$

The following considerations are applied to obtain the variables in dimensionless form:

$$X = \frac{x}{D_h}, \quad Y = \frac{y}{D_h} \quad \text{and} \quad \phi = \frac{\alpha \cdot (T_{wm} - T_f)}{U_b \cdot D_h^2 \cdot \left(\frac{dT_b}{dz} \right)} \quad (20), (21) \text{ and } (22)$$

Replacing Equation (14), Equation (15), Equation (20) up to (22) in Equation (19), dimensionless energy equation for SED and GGDH becomes, respectively:

$$\frac{\partial}{\partial X} \left\{ (\alpha + \alpha_t) \frac{\partial \phi}{\partial X} \right\} + \frac{\partial}{\partial Y} \left\{ (\alpha + \alpha_t) \frac{\partial \phi}{\partial Y} \right\} - (D_h) \left(U \frac{\partial \phi}{\partial X} + V \frac{\partial \phi}{\partial Y} \right) = - \frac{W}{U_B} \alpha \left(\frac{\phi}{\phi_B} \right) \quad (23)$$

$$\begin{aligned} & \frac{\partial}{\partial X} \left[(\alpha_{ex}) \frac{\partial \phi}{\partial X} \right] + \frac{\partial}{\partial Y} \left[(\alpha_{ey}) \frac{\partial \phi}{\partial Y} \right] - D_h \left(U \frac{\partial \phi}{\partial X} + V \frac{\partial \phi}{\partial Y} \right) = - \frac{W}{U_B} \alpha \left(\frac{\phi}{\phi_B} \right) - C_t \frac{\partial}{\partial X} \left[\Gamma_x \frac{\partial \phi}{\partial Y} \right] \\ & - C_t \frac{\partial}{\partial Y} \left[\Gamma_y \frac{\partial \phi}{\partial X} \right] \end{aligned} \quad (24)$$

The fluid temperature field “ T_f ” can be replaced by “ T_b ” and the Equation (22) can be expressed as:

$$\phi_b = \frac{\alpha \cdot (T_{wm} - T_b)}{U_b \cdot D_h^2 \cdot \left(\frac{dT_b}{dz} \right)}, \text{ and } T_b = T_{wm} - \frac{D_h^2 \cdot U_b}{\alpha} \cdot \frac{dT_b}{dz} \cdot \phi_b \quad (25) \text{ and } (26)$$

From Equation (21), the Equation (26) is obtained, and applying this in Equation (17), one gets Equation (28):

$$T_f = T_{wm} - \frac{\phi \cdot U_b \cdot D_h^2 \cdot \left(\frac{dT_b}{dz} \right)}{\alpha}, \text{ and } T_b = T_{wm} - \frac{D_h^2}{\alpha \cdot A} \cdot \frac{dT_b}{dz} \cdot \iint W \cdot \phi \cdot dx \cdot dy \quad (27) \text{ and } (28)$$

Replacing Equation (27) in Equation (24), and using also Equations (19) and (20), the dimensionless bulk temperature is obtained:

$$\phi_b = \frac{D_h^2}{A \cdot U_b} \cdot \iint W \cdot \phi \cdot dX \cdot dY \quad (29)$$

It is possible to compute the heat transfer rate per unit length on the wall surface, “ q' ”, Equation (30). It depends on values for “ T_{wm} ”, “ T_b ”, and on the average heat convection coefficient, “ \bar{h} ”. From fluid enthalpy derivative gradient [$dh_b = c_p \cdot dT_b$], the heat transfer rate per unit length in the fluid, “ q'_f ”, can be expressed by Equation (31).

$$q' = P_e \cdot \bar{h} \cdot (T_{wm} - T_b), \text{ and } q'_f = \rho \cdot U_b \cdot A \cdot c_p \cdot \frac{dT_b}{dz} \quad (30) \text{ and } (31)$$

When Equation (30) is made equal to (31), integrating two cross sections (inlet, namely z_1 , and outlet, namely z_2), it is possible to develop the resulting expression, Equation (32).

$$T_{b_{z_2}} = T_{wm} - (T_{wm} - T_{b_{z_1}}) \cdot e^{-\left(\frac{P_e}{2A} \right) \cdot \frac{\alpha}{U_b} \cdot Nu \cdot (z_1 - z_2)} \quad (32)$$

From Equation (32), the bulk temperature longitudinal (z -axis) variation “ ΔT_b ” is obtained. It is done by “cutting” the duct into a lot of segments and applying the numerical method to find “ ΔT_b ” at each finite cross section. For a given bulk temperature at the duct inlet section (T_{b1}), after solving the equation system, duct outlet bulk temperature (T_{b2}) is computed from that expression, Equation (32). The Dimensionless boundary conditions are given by the following equations:

$$\phi(0, Y) = \frac{\alpha \cdot (T_{wm} - T_1)}{U_b \cdot D_h^2 \cdot \left(\frac{dT_b}{dz} \right)}, \text{ and } \phi(X, 0) = \frac{\alpha \cdot (T_{wm} - T_2)}{U_b \cdot D_h^2 \cdot \left(\frac{dT_b}{dz} \right)} \quad (33)$$

$$\phi(D/D_h, Y) = \frac{\alpha \cdot (T_{wm} - T_3)}{U_b \cdot D_h^2 \cdot \left(\frac{dT_b}{dz} \right)}, \text{ and } \phi(X, L/D_h) = \frac{\alpha \cdot (T_{wm} - T_4)}{U_b \cdot D_h^2 \cdot \left(\frac{dT_b}{dz} \right)} \quad (34)$$

When considering uniform wall temperature, Equation (33) and Equation (34) are equal to zero, and for these particular conditions, it is possible to notice that these boundary conditions are not functions of “ dT_b/dz ”. That simplification becomes equal to the one studied by Patankar (1991). Equations (25),(26) and (27), as well as the boundary conditions from Equations (33) and (34), form a set of differential equations, in which “ ϕ ” and “ dT_b/dz ” parameters are unknown. When that equation system is solved, it is possible to obtain “ T_f ”.

3.3.4. Additional Equations

Additional equations were utilized for the calculation of the factor of friction Moody, f ; coefficient of friction of Fanning, C_f ; Prandtl law; local Nusselt number for the Low Reynolds formulation (Rokni, 2000), Nu_{xp} and Correlation of Gnielinsky, Nu , respectively; these equations are given by:

$$f \equiv \frac{-(dP/dz)D_h}{\rho U_B^2/2}, C_f = \frac{f}{4}, \frac{1}{\sqrt{f}} = 2 \log(\text{Re} \sqrt{f}) - 0.8, Nu_{xp} = D_h \frac{(T_w - T_p)}{\eta(T_w - T_b)} \quad \text{and}$$

$$Nu = \left[\frac{(f/8)(\text{Re}-1000)\text{Pr}}{\left(1 + 12.7(f/8)^{1/2}(\text{Pr}^{2/3} - 1)\right)} \right] \quad (35),(36),(37),(38) \text{ and } (39)$$

4. Numerical Implementation

After applying the method of finite differences to the algebraic equations, to obtain the temperature fields, the following five steps indicate the developed methodology in the numerical solution. (Garcia, 1996):

Step 1: To define the function value of the non uniform temperatures in the walls of the duct $T_{wm} = f(T_1(0, y), T_2(x, 0), T_3(D, y), T_4(x, L))$, what that can be expressed by a Fourier expansion;

Step2: To obtain velocity field and estimated values for “ U_b ” “ T_{wm} ” and “ dT_b/dz ”;

Step 3: Equations for the boundary conditions are evaluated (Equations 33 and 34);

Step 4: Dimensionless energy equation (Temperature field, “ θ ”) at Equation (24) is solved and “ θ_b ” is computed according to Equation (30), until convergence is obtained ($\theta_b < \text{tolerance}$). This is the end of the first iterative loop;

Step 5: A value for “ dT_b/dz ” is computed in accordance with Equation (25). Boundary conditions are updated (step 3) to obtain a solution for the new temperature field (step 4), until convergence is obtained ($dT_b/dz < \text{tolerance}$). This is the end of the second iterative loop;

For all steps, “tolerance of 10^{-7} ” is the value to be accomplished by the convergence criteria, which is applicable to “ θ_b ” (dimensionless bulk temperature), “ dT_b/dz ” and “ θ ” (dimensionless temperature field).

The above procedure is applied for contours of variable temperatures.

5. Results and Discussion

5.1 Fluid Flow and Heat Transfer Field

The Figure 2(a) shows the utilized grid (120X120) in the numerical simulation for the formulations of Low Reynolds, the Figure 2(b) it represents the secondary flow contours and comparisons of the velocity profile (NLEVM, Assato 2001) with the experimental work of the Melling and Whitelaw (1997) for fluid water and $\text{Re}=42000$.

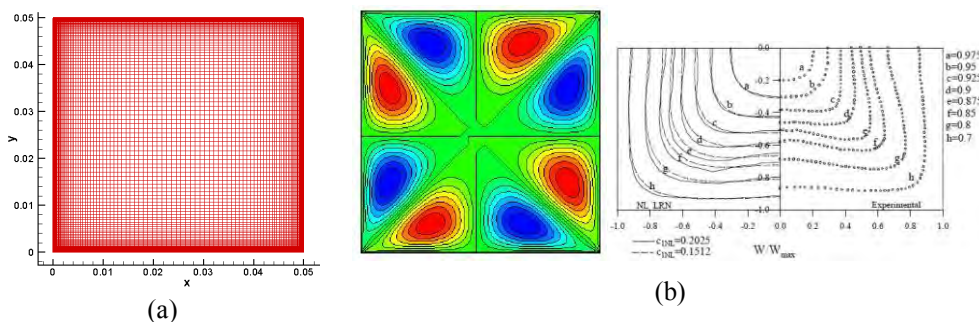


Figure 2: (a) Grid 120X120 for numerical simulation (b) Secondary flow contours and comparisons of the axial mean velocity with Melling and Whitelaw (1973) for water utilizing NLEVM Model

The predicted distributions of the friction coefficient (NLEVM and RSM) and Nusselt number (SED and GGDH) dependence on Reynolds number for fully developed flow and heat transfer in a square duct is shown in Figure 3(a) and 3(b), respectively.

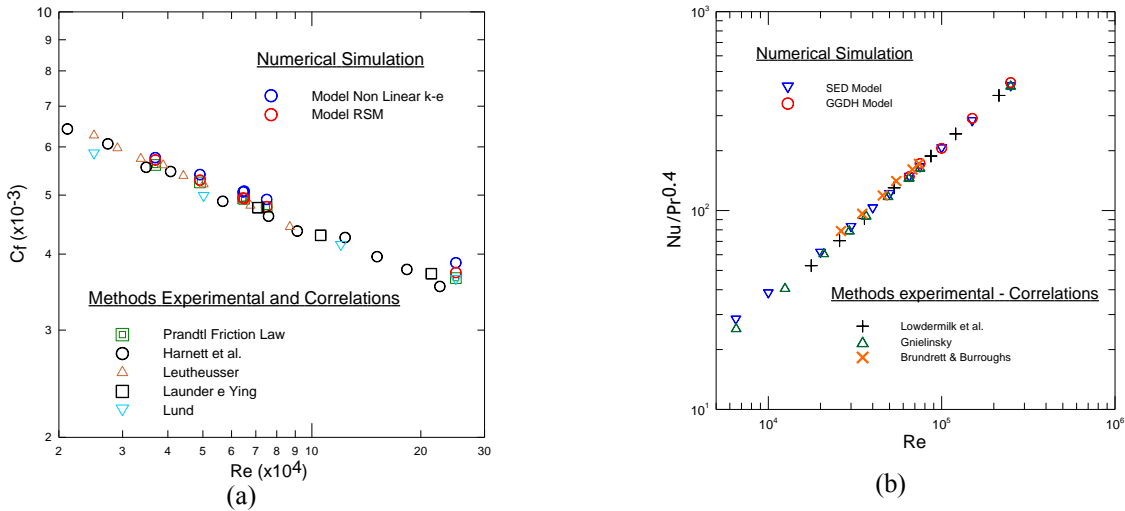


Figure 3: (a) Friction coefficient for fully developed flow, (b) Nusselt number dependence on Reynolds number for fully developed flow

Figure 4(a): comparisons of the Results (RSM-SED) numerical with the experimental for temperature profile (wall constant temperature) $(T_{wm} - T_f)/(T_{wm} - T_C)$ with fluid air and $Re=65000$ (Hirota, 1997) are shown, the figure 4(b) shows the variation of the temperature profile with non-uniform wall Temperature: south=400K, north=373K, east=393K, west=353K; it called of Case I.

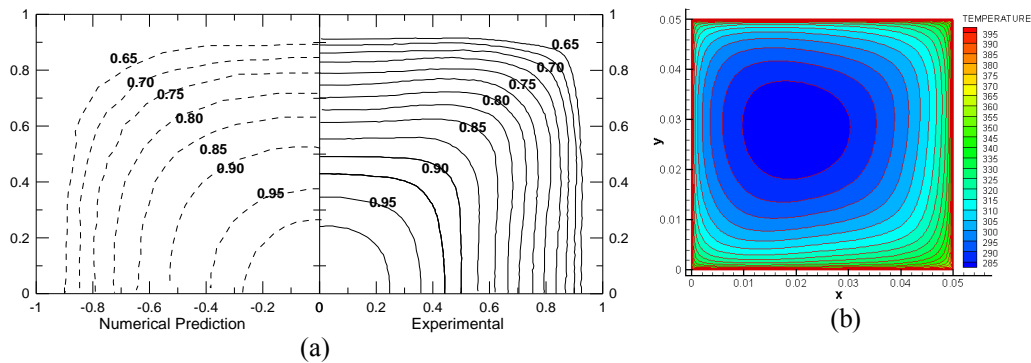


Figure 4: (a) Results (RSM-SED) numerical and (Hirota et al [15]) experimental for mean temperature (uniform wall temperature) (b) Fluid temperature with non-uniform wall Temperature (Case I).

Already the Figure 5(a) shows: The variation of the temperature profile with non-uniform wall temperature, this it is represented by means of functions sine (Case II), south= $(350-20\sin(\zeta))K$, north= $(400-50\sin(\zeta))K$, east= $(330+20\sin(\zeta))K$, west= $(350+50\sin(\zeta))K$. where ζ is function of the radians $(0-\pi/2)$ and i, j (points number of the grid in the direction x and y , respectively). The Figure 5(b) represent the behavior of the “ T_b ” and “ DTb/dz ” for different square cross-sectional sections along of the direction of the main flow, according to Equation (31).

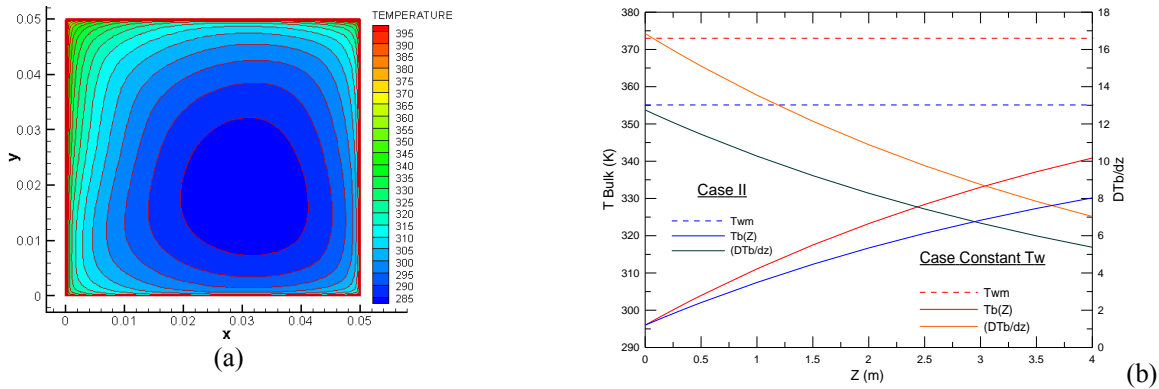


Figure 5: (a) Fluid temperature with non-uniform wall temperature (Case II) (b) Behavior “ T_b ” for different square cross-sectional sections and cases throughout of the direction of the main flow.

The Figures 6 (a) e (b), shown the temperature distribution for a rectangular duct of the aspect ratio(1:2) represented also by means of functions sine (Case II). Exist a third case denominated Case III, it is represented by:

$$\text{south} = 405 + 10 \left[\frac{nx - 1}{nx_{\text{m\acute{a}x}} - 1} \right] K; \quad \text{North} = 395 + 10 \left[\frac{nx - 1}{nx_{\text{m\acute{a}x}} - 1} \right] K; \quad \text{east} = 405 - 10 \left[\frac{ny - 1}{ny_{\text{m\acute{a}x}} - 1} \right] K;$$

$$\text{west} = 415 - 10 \left[\frac{ny - 1}{ny_{\text{m\acute{a}x}} - 1} \right] K, \text{ where some results for rectangular ducts will be shown in the Table I.}$$

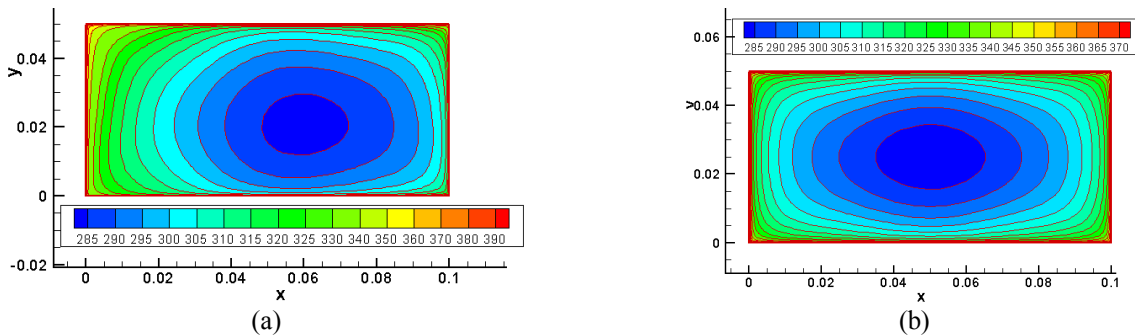


Figure 6: (a) Rectangular duct of aspect ratio (1:2) case II, $Re=65000$ with $T_b=300$ K, utilizing the SED model (b) Rectangular duct of aspect ratio (1:2) with constant temperature in the perimeter $T_{wm}=373$ K, $Re=65000$ with $T_b=300$ K, utilizing the SED model.

Garcia (1996) analyzed the laminar flow with the coupled of the conduction and radiation in rectangular ducts and concluded that as increases the aspect ratio, the Nusselt number found for the coupling (non uniform temperature), differs from that found for ducts with constant temperature imposed around the perimeter of the section. That shows that would be admissible to make a mistake in the case of using literature results without calculating the energy equation.

In the present work, the variations of the average Nusselt number for a square duct and different cases analyzed (uniform and non uniform temperature in the perimeter) are minimal. Already in the case of rectangular duct with an aspect ratio (1:2), the variations should be taken into account as shown in Table 1.

Table 1. Numerical results obtained through RSM-SED model (Rivas, 2010), for the averaged Nusselt number in a rectangular duct with aspect of ratio (1:2).

Cases Analyzed	Reynolds number (Re)	Nusselt number calculated (Nu)	Correlation Dittus Boelter (Nu).
Temperature Constant	65000	145, 910	142,89
Case II	65000	139, 682	-

Case III	65000	145, 059	-
Temperature Constant	28853	79, 101	77,1
Case III	28853	76, 769	-

5.2 Heat conduction coupled to turbulent forced convection

The Figure 7 shows, the grid non-uniform utilized for the coupled solid-fluid.

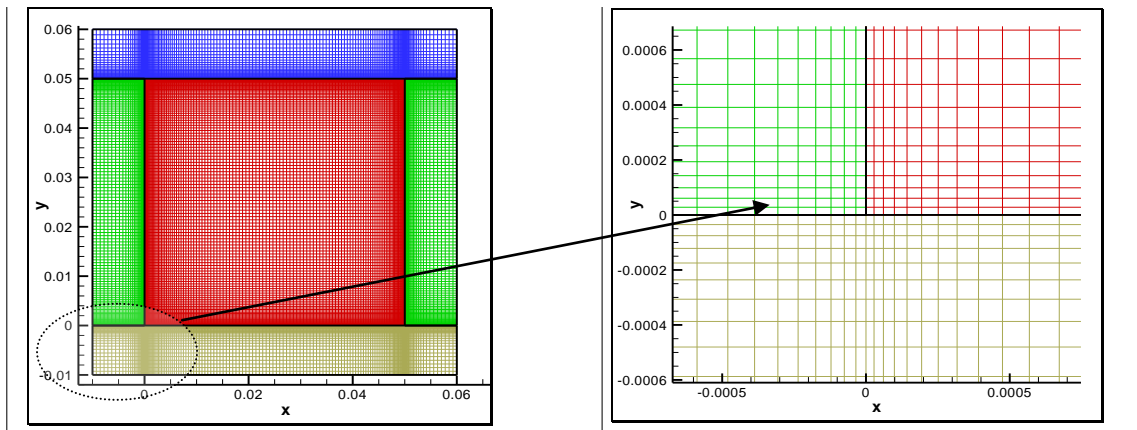


Figure 7. Grid non-uniform coupled solid-fluid

The figure 8 shows below, different cases for the temperatures prescribed in the external contour of the plates coupled (solid), the case (a) shows constant temperatures in the all external contour of 373K, (b) different temperatures in the face North=600K, south=500K, east and west 373K and the case (c) shows a example qualitative representing the versatility of the program to work with different thermal conductivities, (Rivas, 2010).

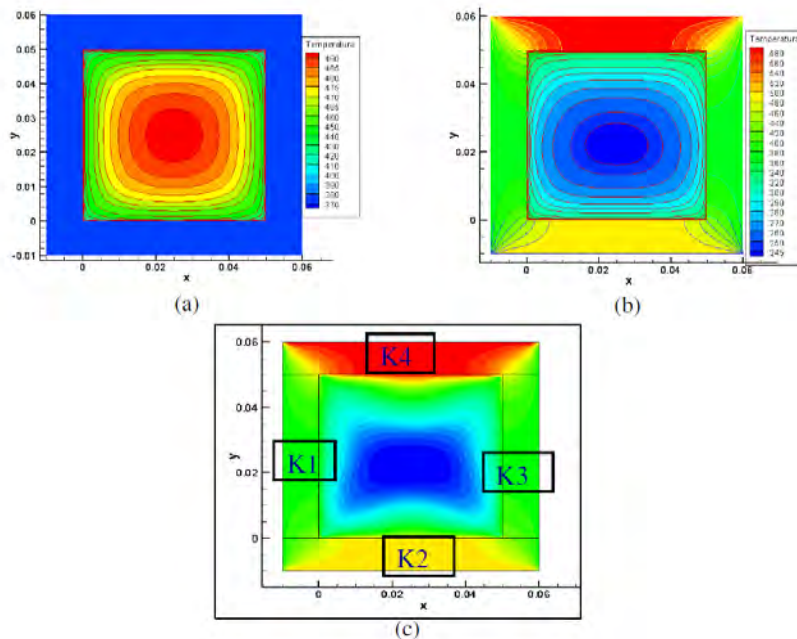


Figure 8. Coupled solid-fluid with prescribed conditions (a) external temperatures $T_{ext}=373K$; (b) different temperatures in the face North=600K, south=500K, east and west 373K, (c) example qualitative representing the versatility of the program to work with different thermal conductivities.

6. Conclusions

The results presented for the friction factor and Nusselt number in function of a large range of the Reynolds number for uniform wall temperature present good agreement with the experimental works and correlation of the literature, (Figure 3(a), (b)) using the turbulent convective heat transfer proposed. Figures 4(b) and 5(a) show new results investigated in present work, note a distortion of the temperatures field and as consequence the variation of the Nusselt number caused mainly by the distribution of the non-uniform wall temperature (Case I and II, with fluid air and $Re=65000$, respectively). Most applications can be approximated by the functions sine and cosine in the wall, but we are able to resolve by means of the methodology presented, any peripheral heat flux variation that can be expressed by a Fourier expansion (Kays and Crawford [30]). The Figure 5(b) shows the comparisons of the behavior of the curves " T_b " and " DT_b/dz " to the long of the main direction of the flow for Case II and Case uniform wall temperature. The variations of the average Nusselt number for a square duct and different cases analyzed (uniform and non uniform temperature in the perimeter) are minimal. Already in the case of duct with an aspect ratio (1:2) the variations should be taken into account. These results can be helpful in the project of thermal devices as in heat transfer and secondary flows in cavities, seals, channel of gas turbines and others. The coupled solid fluid represent good qualitative results.

7. REFERENCES

Assato, M. 2001. *Análise numérica do escoamento turbulento em geometrias complexas usando uma formulação implícita*, Doctoral Thesis, Departamento de Engenharia Mecânica, Instituto Tecnológico de Aeronáutica - ITA, São José dos campos - SP, Brazil, 2001.

Assato, M., De Lemos, M.J.S. 2009. Turbulent flow in wavy channels simulated with nonlinear models and a new implicit formulation, *Numerical Heat Transfer – Part A: Applications*. 56 (4) (2009) 301-324.

Campo, A., Tebeest, K., Lacoa, U., Morales, J.C. 1996. Application of a finite volume based method of lines to turbulent forced convection in circular tubes, *Numerical Heat Transfer – Part A: Applications*. 30 (5) (1996) 503-517.

Emery, A.F., Neighbors P.K. and Gessner, F.B. 1980. The numerical prediction of developing turbulent flow and heat transfer in a square duct, *Journal Heat Transfer*, 102 (1980) 51–57.

Ergin, S.M., Ota, Yamaguchi, 2001. Numerical study of periodic turbulent flow through a corrugated duct, *Numerical Heat Transfer – Part A: Applications*. 40 (2) (2001) 139-156.

Garcia, E.C., 1996. *Condução, convecção e radiação acopladas em coletores e radiadores solares*, Doctor degree thesis, ITA - Instituto Tecnológico de Aeronáutica, São José dos Campos, SP, Brasil.

Gessner, F.B. and Emery, A.F., 1976. "A Reynolds stress model for turbulent corner flows – Part I: Development of the model", *Journal Fluids Eng.* 98 (1976) 261-268.

Gessner, F.B. and Po, J.K. 1976. " A Reynolds stress model for turbulent corner flows – Part II: Comparison between theory and experiment ", *Journal Fluids Eng.* 98 (1976) 269-277.

Hirota, M., Fujita, H., Yokosawa, H., Nakai, H., Itoh,H.,1997.Turbulent heat transfer in a square duct, *International Journal Heat and fluid flow*, 18 (1997) 170-180.

Home, D., Lightstone, M.F., Hamed, M.S., 2009. Validation of DES-SST based turbulence model for a fully developed turbulent channel flow problem, *Numerical Heat Transfer – Part A: Applications*. 55 (4) (2009) 337-361.

Hongxing, Y., 2009. Numerical study of forced turbulent heat convection in a straight square duct, *International Journal of Heat and Mass Transfer*, 52 (2009) 3128-3136.

Kays, W.M. and Crawford, M. 1980. *Convective Heat and Mass Transfer*, McGraw-Hill, New York, USA, 1980, pp. 250-252.

Lauder, B.E. and Ying, W.M., 1973. "Prediction of flow and heat transfer in ducts of square cross section", *Proc. Inst. Mech. Eng.*, 187 (1973) 455-461.

Luo, D. D., Leung, C.W., Chan, T.L., Wong, W.O., 2005. Simulation of turbulent flow and forced convection in a triangular duct with internal ribbed surfaces, *Numerical Heat Transfer – Part A: Applications*. 48 (5) (2005) 447-459.

- Melling, A. and Whitelaw, J.H. 1976. " Turbulent flow in a rectangular duct ", *Journal Fluid Mechanical*. 78 (1976) 289-315.
- Moran, M. J. et al., *Introdução à Engenharia de Sistemas Térmicos: Termodinâmica, Mecânica dos Fluidos e Transferência de Calor*, LTC Ed., Rio de Janeiro-RJ, Brasil, 2005.
- Myon, H.K. and Kobayashi, T. 1991. Numerical Simulation Of Three Dimensional Developing Turbulent Flow in a Square Duct with the Anisotropic κ - ϵ Model, *Advances in Numerical Simulation of Turbulent Flows ASME, Fluids Engineering Conference*, 1991. Vol.117, Portland, United States of America, pp. 17-23.
- Nakayama, A., Chow, W.L. and Sharma, D. 1983. Calculation of fully development turbulent flows in ducts of arbitrary cross-section, *Journal Fluid Mechanical*, 128 (1983) 199-217.
- Nikuradse, J. 1926. "Untersuchung uber die Geschwindigkeitsverteilung in turbulenten Stromungen", *Diss. Göttingen, VDI - forschungsheft* 281.
- Park, T.S. 2004. Numerical study of turbulent flow and heat transfer in a convex channel of a calorimetric rocket chamber, *Numerical Heat Transfer – Part A: Applications*. 45 (10) (2004) 1029-1047.
- Patankar, S.V., *Computation of Conduction and Duct Flow Heat Transfer*, Innovative Research, Maple Grove, USA, 1991.
- Qin, Z.H., Plechter, R.H. 2006. "Large eddy simulation of turbulent heat transfer in a rotating square duct", *International Journal Heat Fluid Flow*. 27 (2006) 371-390.
- Rivas Ronceros, G.A., 2010. *Simulação numérica da convecção forçada turbulenta acoplada à condução de calor em dutos retangulares*, Doctor degree thesis, ITA - Instituto Tecnológico de Aeronáutica, São José dos Campos, SP, Brasil.
- Rokni, M. 1998. Numerical investigation of turbulent fluid flow and heat transfer in complex duct, *Doctoral Thesis, Department of Heat and Power Engineering. Lund Institute of Technology, Sweden*, 1998.
- Rokni, M., 2000. A new low-Reynolds version of an explicit algebraic stress model for turbulent convective heat transfer in ducts, *Numerical Heat Transfer – Part B: Fundamentals*. 37 (3) (2000) 331-363.
- Rokni, M., Sundén, B., 1996. Numerical investigation of turbulent forced convection in ducts with rectangular and trapezoidal cross section area by using different turbulence models, *Numerical Heat Transfer – Part A: Applications*. 30 (4) (1996) 321-346.
- Saidi, A., Sundén, B., 2001. " Numerical simulation of turbulent convective heat transfer in square ribbed ducts", *Numerical Heat Transfer – Part A: Applications*. 38 (1) (2001) 67-88.
- Sharatchandra, M.C., Rhode, D.L., 1997. Turbulent flow and heat transfer in staggered tube banks with displaced tube rows, *Numerical Heat Transfer – Part A: Applications*. 31 (6) (1997) 611-627.
- Speziale, C.G., 1987. "on non linear k-l and k-e models of turbulence, *Journal Fluid Mechanical*"., v.178, p. 459-475, 1987.
- Su, J., Da Silva Neto, A.J., 2001. Simultaneous estimation of inlet temperature and wall heat flux in turbulent circular pipe flow, *Numerical Heat Transfer – Part A: Applications*. 40 (7) (2001) 751-766.
- Valencia, A., 2000. Turbulent flow and heat transfer in a channel with a square bar detached from the wall, *Numerical Heat Transfer – Part A: Applications*. 37 (3) (2000) 289-306.
- Yang, G., Ebadian, M.A., 1991. Effect of Reynolds and Prandtl numbers on turbulent convective heat transfer in a three-dimensional square duct, *Numerical Heat Transfer – Part A: Applications*. 20 (1) (1991) 111-122.
- Yang, Y.T., Hwang, M.L. 2008. Numerical simulation of turbulent fluid flow and heat transfer characteristics in a rectangular porous channel with periodically spaced heated blocks, *Numerical Heat Transfer – Part A: Applications*.

G. Rivas, E. Garcia and M. Assato
Numerical Simulation of Turbulent Forced Convection Coupled to Heat Conduction in Square Ducts

54 (8) (2008) 819-836.

Zhang, J., Dong, L., Zhou, L., Nieh, S. 2003. Simulation of swirling turbulent flows and heat transfer in a annular duct, Numerical Heat Transfer – Part A: Applications. 44 (6) (2003) 591-609.

Zheng, B., Lin, C.X., Ebadian, M.A., 2003. Combined turbulent forced convection and thermal radiation in a curved pipe with uniform wall temperature, Numerical Heat Transfer – Part A: Applications. 44 (2) (2003) 149-167.

8. RESPONSIBILITY NOTICE

The author(s) is (are) the only responsible for the printed material included in this paper.